Electronic Supplementary Material (ESI) for Environmental Science: Processes & Impacts.

Supporting Information for

Evaluating parameter availability for physiologically based pharmacokinetic (PBPK) modeling of perfluorooctanoic acid (PFOA) in zebrafish.

Manoochehr Khazaee and Carla A. Ng*

University of Pittsburgh, Department of Civil and Environmental Engineering, 3700 O'Hara St, Pittsburgh, PA, 15261.

*Corresponding author: carla.ng@pitt.edu

S1. Parameter Glossary

BW: Body weight

LW: Liver weight

MW: Muscle weight

VL: Liver volume

VM: Muscle volume

VK: Kidney volume

VA: Adipose volume

VB: Blood volume

VG: Bile volume

VLF: Fluid liver volume

VKF: Fluid kidney volume

VMF: Fluid muscle volume

VAF: Fluid adipose volume

AL: Liver surface area

AL: Liver surface area

AK: Kidney surface area

AM: Muscle surface area

AA: Adipose surface area

AB: Gallbladder surface area

AG: Gill surface area

QBi: Biliary flow rate

QW: Gill ventilation rate

QB: Blood flow rate

QBL: Liver blood perfusion rate

QBK: Kidney blood perfusion rate

QBM: Muscle blood perfusion rate

QBA: Adipose blood perfusion rate

CPB: Plasma protein concentrations

CFABPLT: FABP concentrations in liver

CPL: Liver fluid protein concentrations

CPK: Kidney fluid protein concentrations

CPM: Muscle fluid protein concentrations

CPA: Adipose fluid protein concentrations

b_{uptake}: Liver active uptake rate

b_{clear}: Liver active clearance rate

K_P: Plasma protein association constants

K_{FABP}: FABP association constants

P_{eff}: Effective membrane permeability

CR_{SS}^{C-W} : Steady-state cell-water concentration ratio

k^{W-B}: Water to blood uptake rate constant

k^{B-W}: Rate constant for diffusion from blood back to water

r : Radius

S2.PFOA Mass Balance Equations and Mass Transfer Coefficients

We calculated the rate constant for gill uptake (k^{W-B}) by using the following equation (1):

$$k^{W-B} = \left(\frac{1}{Q_W} + \frac{1}{P_{eff}A^{B-W}}\right)^{-1}$$

As noted above, A^{B-W} is equal to gill surface area of zebrafish representing the area for blood-water exchange. To calculate rate constant for diffusion from blood back to water (k^{B-W}), we employed proposed equation from Ng et al. (2013) as below (1):

$$k^{B-W} = \frac{k^{W-B}}{CR_{SS}^{C-W}}$$

The exchange and interactions between protein and PFOA are listed in Table S1. Mass transfer coefficients were extracted from the Ng et al. (2013) (1). Uptake and loss rate constants from water to blood and from blood to water were calculated as follows:

$$b^{W-B} = k^{W-B}$$

$$B^{B-W} = \frac{K^{B-W}}{VB}$$

In order to find the rate constant of internal transfer among compartments, we employed the mass transfer coefficient as below:

$$k^{B-iF} = \left(\frac{1}{Q_B^i} + \frac{1}{P_{eff}A^{B-iF}}\right)^{-1}$$

Similar overall resistance is assumed ($k^{iF-B} = k^{B-iF}$) for diffusion from the interstitial fluid back to blood.

The rate constant determined by dividing the value of k^{B-iF} over the volume respective compartment:

$$b^{B-iF} = \frac{K^{B-iF}}{VB}$$

$$b^{iF-B} = \frac{K^{B-iF}}{V^{iF}}$$

For transport from fluid parts to tissues sub-compartments, only the membrane permeability provides a resistance to transport. Therefore, the mass transfer coefficient is :

$$K^{iF-iT} = P_{eff}A^{iF-iT}$$

Finally, the rate constant for diffusion from interstitial fluid to tissues sub-compartments and from tissues sub-compartments to interstitial fluid were easily calcuated as below :

$$b^{iF-iT} = \frac{K^{iF\_LT}}{V^{iF}}$$

$$b^{iT-iF} = \frac{K^{iT\_LF}}{V^{iT}}$$

The sum of transport with NTCP and OSTα/β mediated proteins is considered for for uptake.

$$b_{uptake=b_{OST\alpha/\beta}+b_{NTCP}}$$

Moreover, for clearance, the value of ASBT transporter protein is used.

$$b_{clear} = b_{ASBT}$$

By dividing the biliary flow rate over the volume of biliary system, the rate constant for biliary removal was calculated:

$$b_{Bi} = \frac{QBi}{VG}$$

Furthermore, the PFOA mass balance equations for compartments involved in the model depicted in Table S1.

Table S1. PFOA Mass Balance Equations

Liver Fluid (LF)

$$\frac{dM_{free}^{LF}}{dt} = b_{Uptake}^{B-LF}M_{free}^{B} + b^{B-LF}M_{free}^{B} + b^{LT-LF}M_{free}^{LT} - (b^{LF-B}M_{free}^{LT} + b^{LF-LT})M_{free}^{LF} - b_{on}^{LF}M_{free}^{LF} + b_{off}^{LF}M_{bound}^{LF}$$

$$\frac{dM_{bound}^{LF}}{dt} = b_{on}^{LF}M_{free}^{LF} - b_{off}^{LF}M_{bound}^{LF}$$

Liver Tissue (LT)

$$\frac{dM_{free}^{LT}}{dt} = b^{LF-LT}M_{free}^{LF} + b^{Bi-LT}M_{free}^{Bi} - (b_{clear}^{LT-Bi} + b^{LT-Bi} + b^{LT-LF})M_{free}^{LT} - b_{on}^{LT}M_{free}^{LT} + b_{off}^{LT}M_{bound}^{LT}$$

$$\frac{dM_{bound}^{LT}}{dt} = b_{on}^{LT}M_{free}^{LT} - b_{off}^{LT}M_{bound}^{LT}$$

Blood (B)

$$\frac{dM_{free}^{B}}{dt} = b^{W-B}C_{free}^{W} - b^{B-W}M_{free}^{B} - \sum_{i} b^{B-iF}M_{free}^{B} + \sum_{i} b^{LT-B}M_{free}^{LT} - b_{on}^{B}M_{free}^{B} + b_{off}^{B}M_{bound}^{B}$$

$$\frac{dM_{bound}^{B}}{dt} = b_{on}^{B}M_{free}^{B} - b_{off}^{B}M_{bound}^{B}$$

Bile (Bi)

$$\frac{dM_{free}^{Bi}}{dt} = b_{clear}^{LT-Bi}M_{free}^{LT} - b^{Bi-LT}M_{free}^{Bi} + b^{LT-Bi}M_{free}^{LT} - \frac{Q_{Bi}}{V_{Bi}}M_{free}^{Bi}$$

Muscle Fluid (MF)

$$\frac{dM_{free}^{MF}}{dt} = b^{B-MF}M_{free}^{B} - b^{MT-MF}M_{free}^{MT} - (b^{MF-B}M_{free}^{B} + b^{MF-MT})M_{free}^{MF} - b_{on}^{MF}M_{free}^{MF} + b_{off}^{MF}M_{bound}^{MF}$$

Muscle Tissue (MT)

$$\frac{dM_{free}^{MT}}{dt} = b^{MF-MT}M_{free}^{MF} - b^{MT-MF}M_{free}^{MT}$$

Adipose Fluid (AF)

$$\frac{dM_{free}^{AF}}{dt} = b^{B-AF}M_{free}^{B} - b^{AT-AF}M_{free}^{AT} - (b^{AF-B}M_{free}^{B} + b^{AF-AT})M_{free}^{AF} - b_{on}^{AF}M_{free}^{AF} + b_{off}^{AF}M_{bound}^{AF}$$

Adipose Tissue (AT)

$$\frac{dM_{free}^{AT}}{dt} = b^{AF-AT}M_{free}^{AF} - b^{AT-AF}M_{free}^{AT}$$

Kidney Fluid (KF)

$$\frac{dM_{free}^{KF}}{dt} = b^{B-KF}M_{free}^{B} - b^{KT-KF}M_{free}^{KT} - (b^{KF-B}M_{free}^{B} + b^{KF-KT})M_{free}^{KF} - b_{on}^{KF}M_{free}^{KF} + b_{off}^{KF}M_{bound}^{KF}$$

Kidney (KT)

$$\frac{dM_{free}^{KT}}{dt} = b^{KF-KT}M_{free}^{KF} - b^{KT-KF}M_{free}^{KT}$$

S3. Derivation of Model Parameters

S3.1 Physiological Parameters

S3.1.1 Body weight

Since gender differences have been reported in the toxicokinetics of PFOA in different fish species, we consider parameter availability for both genders (2–5). The weight of adult zebrafish was reported between 0.2 to 0.9 g (6–10). Zang et al. (2013) indicated that the average weight of male and female adult zebrafish is 0.41 and 0.82 g, respectively (8). Accordingly, we considered a 0.41 g adult male, 0.82 g adult female, and a 0.6 g adult zebrafish (average of male and female) for our model-based parameter evaluation.

S3.1.2 Tissue Volumes

Although the volume of a particular tissue is a relatively basic property, a wide variety of methods for estimating volume has been used in the literature, including planimetry, paper weighing, lineal analysis, random point analysis, biomolecular imaging, water displacement volumetry, tape measurements, and CT or MRI scans (11–15). Here we present available estimates for zebrafish tissues by different techniques, and summarize the collected values (including ranges, where appropriate) for our representative male, female, and average adult zebrafish in Table S2. For most of the tissues considered, no direct measurements were available and values were estimated based on other properties, such as weight of tissues. Final values of all volumes used in the model are listed in Table S2.

Liver

Örn et al. (1998) measured the liver weight of adult female zebrafish as equal to 4.3 mg, which represents 1.83% of the total zebrafish body weight (6). More recently, Cheng et al. (2016) indicated that liver weight is ~2.10% and ~4.51% of total male and female zebrafish body

weights, respectively. Based on the Cheng et al. (2016) study, we calculated the liver weight as a fraction of body weight for male, female, and adult zebrafish, as equal to approximately 0.008 g, 0.036 g, and 0.019 g, respectively (14). If we instead use the Örn et al. (1998) estimate, the liver weight would be 0.007 g, 0.015 g, and 0.01 g for male, female, and adult zebrafish, respectively. Based on this weight, we can either calculate the volume of the liver by assuming fish density equal to 1 g/ml. Cheng et al. (2016) also estimated directly the volume of adult zebrafish liver as $0.535mm^3$ (14).

Biliary system

For the bile volume, we found only an estimate of the zebrafish biliary system volume from the Cheng et al. (2016) study, which states that 18% of the zebrafish liver volume comprises the biliary system. In our model, we used the same value for both genders, based on this 18% value and on the directly estimated volume of adult zebrafish liver (Table S2) (14).

Muscle

Johnston et al. (2011) reported that muscle tissue represents 60% of the total adult zebrafish body weight (16). Similar to the liver compartment (assuming fish density equal to 1 g/ml) the volume of the muscle compartment was estimated as 0.36 ml, 0.49 ml, and 0.24 ml for adult, female, and male, respectively.

Kidney

We estimated the volume of the kidney based on the volume of the glomerulus. According to McCampbell et al. (2015), adult zebrafish at 6 months have approximately 450 nephrons (each nephron has one glomerulus) (17). Accordingly, there are 450 glomeruli in the kidney of adult zebrafish. Zhou and Hildebrandt (2012) determined that one glomerulus contained 42 podocytes

and the volume of each podocyte is 7709 μm^3 (18). Consequently, we calculated the volume of kidney to be 1.46×10^{-4} ml for adult zebrafish.

Adipose

The volume of adipose was extracted from the control group of the Hasumura et al. (2012) experiment for male and female zebrafish (19). Based on their study, a male zebrafish with a weight of 342.5 mg has 0.81 mm^3 adipose, and a female with the weight of 363.6 mg has 2.8 mm^3 adipose. These values were converted based on the weight of male and female zebrafish used for our model-based evaluation; the average of the values was considered for adult zebrafish.

Blood

The blood volume was extracted from Zang et al. (2013) (8). Based on their results, the mean maximal blood volumes collected from male and female zebrafish were approximately 9 and 17 µl, respectively. We applied the data as a blood volume in our study for different genders and used their average for adult zebrafish in our model.

Table S2. Volume of different compartments (ml)

Compartment	Male	Female	Adult
Liver	5.53×10^{-4}- 8×10^{-3}	5.53×10^{-4} - 0.036	5.53×10^{-4}- 0.019
Muscle	0.24	0.49	0.36
Kidney	1.46×10^{-4}	1.46×10^{-4}	1.46×10^{-4}
Adipose	1.02×10^{-3}	6.32×10^{-3}	3.67×10^{-3}
Blood	9×10^{-3}	17×10^{-3}	13×10^{-3}
Bile	9.95×10^{-5}	9.95×10^{-5}	9.95×10^{-5}

S3.1.3 Volume of Interstitial Fluid Compartments

We have not found any specific data for the interstitial fluid volumes of different zebrafish tissues. To estimate the volume of interstitial fluid sub-compartments, we applied the scaling factors reported by Buschnell et al. (1988) for trout, converted to an estimate for zebrafish using the ratio of the zebrafish and trout body weights (20). They labeled and used EDTA ([^{58}Co] EDTA) as an indicator of the extracellular compartment. Based on the Buschnell et al. (1988), volume of interstitial fluids relative to the weight of organ tissues were estimated for liver, kidney, muscle, and adipose of rainbow trout (V_F/W_T, ml/g) 0.283, 0.672, 0.054, and 0.174, respectively (20). According to these scaling factor the interstitial fluid volumes of liver, muscle, kidney, and adipose were estimated for the model (Table S3).

Table S3. Interstitial fluid volume of different compartments (ml)

Compartment	**VF/WT based on Buschnell et al. (1988)**(20)	**Male**	**Female**	**Adult**
Liver	0.283	1.7×10^{-3}	4.24×10^{-3}	2.83×10^{-3}
Muscle	0.054	0.013	0.026	0.019
Kidney	0.672	1.38×10^{-3}	2.39×10^{-3}	1.81×10^{-3}
Adipose	0.174	1.77×10^{-4}	1.09×10^{-3}	6.38×10^{-4}

S3.1.4 Surface Area of Compartments

In addition to the interstitial fluid volume and tissue volume, the surface area of each compartment also plays a significant role in controlling the rate of inter-compartment chemical exchange (1). Unfortunately, there are no available data in literature for zebrafish tissue surface areas. Therefore, we derived these estimates based on substantial simplifications.

Liver

Based on the assumption that the important space to estimate blood-to-compartment exchange is the total surface area of the capillary bed, and also by considering the information described by

Soldatov (2006), we calculated the liver surface area according to an estimate of capillary surface area (21). This estimate was based on the only available data for the dimensions of red muscle and white muscle capillaries used by Ng and Hungerbühler (2013), and described in detail in their paper (1,21). Soldatov (2006) indicated that in red muscles, capillaries are shorter and thinner (diameter of 9 – 13 μm, length of 470–770 μm), while in white muscles, on the contrary, they are longer and wider (diameter of 50–73 μm, length of 890–1300 μm) (21). We used the average of these dimensions to calculate the area and volume of a single capillary, assuming cylindrical geometry. After that, we used the blood volume in liver of zebrafish to calculate the total number of capillaries. The surface area of liver for male, female, and adult zebrafish was then calculated based on the total number of capillaries and the surface areas of a single capillary (Table 7).

We could not find the blood volume of other compartments. Consequently, we had to change the method for surface area estimation of other compartments. We found the diameter of one cell of each tissue (e.g. glomerulus, hepatocyte, adipocyte, and muscle fiber to estimate the surface area of kidney, liver, adipose, and muscle, respectively). The volume of each cell was then estimated by assuming a spherical shape for hepatocytes, glomeruli, and adipocytes, and a cylindrical shape for muscle fiber (22). In the next step, the number of cells in each tissue was estimated by dividing the volume of each tissue by the volume of the corresponding cell (e.g. volume of liver/volume of hepatocyte). Then, the surface area of each tissue was calculated by multiplying the surface area of one cell by the total number of cells in the tissue. These surface areas take into account the entire tissue, rather than only those in contact with blood vessels, and are therefore likely substantial overestimates of the surface areas for blood-tissue exchange.

Kidney

As described, we calculated the volume of kidney based on the volume of glomerulus, and assuming the kidney contains 450 glomeruli. The glomerular volume estimate corresponds to a diameter of 85 μm, which is close to the average estimation of other studies, 75 μm (23,24). Finally, the surface area of kidney was calculated as follows:

$KA=450 \times 4\pi r^2 = 0.103\ cm^2$

The same value was considered for adult, male, and female of zebrafish.

Muscle

In order to estimate the surface area of the muscle compartment, it was assumed that muscle fiber has a spherical shape and the average diameter of one fiber is around 20 μm in zebrafish (25). The number of fibers in muscle tissue was calculated by dividing the volume of muscle to the volume of one fiber. Then, we estimated the surface area of muscle by multiplying the total number of fibers by the surface area of one fiber.

Adipose

Moreover, similar to muscle and kidney, we found the average diameter of adipocytes and hepatocytes to be 35 and 17 μm in zebrafish, respectively (14,26). Next, the surface area of liver and adipose tissues was calculated by assuming the spherical shape of the cells.

Gallbladder

Grosel et al. (2000) found the surface area of the gallbladder in rainbow trout to be 11 cm^2/kg (27). Accordingly, we calculated the surface area of gallbladder for the zebrafish based on their relative weights. This surface area was used to model passive diffusion between liver and bile.

Gill

We could find neither the surface area of zebrafish gills nor the diameter of the gill lamellae in literature. Therefore, we decided to estimate that by using the ratio of surface area of liver to the surface area of gill from Ng and Hungerbühler (2013) study for trout (1). The liver was chosen as a comparison tissue because we had higher confidence in our value of liver surface area than other tissues for zebrafish. Ng and Hungerbühler estimated the surface area of liver and gill as 16 and 71 cm^2, respectively. Therefore, we multiplied the estimated liver surface area for zebrafish by 4.43 (gill/liver surface area ratio) to obtain the gill surface area.

The surface area of each compartment is presented in Table S4.

Table S4. Surface area of different compartments (m^2)

Compartment	Male	Female	Adult
Liver	1.9×10^{-4}	1.9×10^{-4}	1.9×10^{-4}
Muscle	0.07	0.14	0.11
Kidney	1.03×10^{-5}	1.03×10^{-5}	1.03×10^{-5}
Adipose	1.74×10^{-5}	1.08×10^{-3}	6.28×10^{-4}
Gill	8.59×10^{-4}	8.59×10^{-4}	8.59×10^{-4}
Gallbladder	4.51×10^{-3}	9.02×10^{-7}	6.6×10^{-7}

S3.1.5 Blood Perfusion Rate and Water, Blood, and Biliary Flow Rates

In order to estimate the blood perfusion rate in different compartments, we employed the results of the Barron et al. (1987) and Nichols et al. (1990) studies (28,29) for rainbow trout. Barron et al. (1987) reported that total hepatic blood flow is equal to 2.9% cardiac output (28). Moreover, based on Nichols et al. (1990) the contribution of cardiac output to kidney, muscle and adipose blood flow was assumed to be 5.6 %, 25.2 %, and 8.2 %, respectively (29). The calculated blood perfusion rates for each compartment are shown in Table S5.

For the blood flow rate, we used the estimation of 11.1 µl/min from the Péry et al. (2013) study for 0.5 g zebrafish (30). Thus, the blood flow rate estimation in our model was 19.18, 26.21, and 13.1 ml/day for adult, female, and male, respectively (see Table 1). Since we could not find a specific value for biliary flow rate, we employed the results of Schmit and Weber (1973) for trout (Table 1) (31). The estimated value for adult, male, and female are 1.44×10^{-3}, 1.96×10^{-3}, and 9.84×10^{-4} ml/day, respectively. Péry et al. (2013) estimated the gill ventilation rate for 0.4 g adult cyprinid to be 0.55 mL/min at 27 °C (30). We converted this value based on the weights of male, female, and adult zebrafish in our model.

The final values used for blood perfusion rate of each tissue in our model are listed in Table S5.

Table S5. The blood perfusion rate of compartments (ml/day)

Compartment	Male	Female	Adult
Liver	0.38	0.65	0.55
Kidney	0.73	1.46	1.07
Muscle	3.30	6.60	4.83
Adipose	1.07	2.14	1.57

S3.2 Protein-Related Parameters

S3.2.1 Tissue-Specific Protein Concentrations

Zebrafish has no albumin, dissimilar to human plasma where the albumin is the most abundant protein (32). In the model, it was assumed that other proteins, probably apoliproproteins, perform the same role as albumin (33). As an upper bound, we considered total protein concentrations in plasma, which was reported to be 37.7 mg/ml in males and 53.1 mg/ml in females (33). For adult zebrafish, we used the average protein concentration in plasma of both sexes. Because the value of total protein concentration in plasma was in the unit of mg/ml, it needs to be changed to mol/ml based on the model. Thus, based on the Li et al. (2016) study, we calculated the mean

molecular weight of proteins in zebrafish plasma in order to convert protein concentrations to units of mol/ml for calculations of PFAA-protein binding (33). According to Londraville and Sidell (1996), we estimated the concentration of FABPs in liver tissues as approximately 0.05 mmol/L (34). Due to lack of data, we reviewed both general mammalian and human-focused literature to find the concentrations of albumin in interstitial fluid of different compartments. It was shown that the concentrations of albumin in interstitial fluid of the liver is half of available albumin in plasma (32,35). Thus, we assumed the same ratio in the model, and assume the same value for both liver and kidney. To estimate the concentrations of proteins in interstitial fluid of adipose and muscle, the concentration of total protein in the plasma of zebrafish was multiplied by the ratio of concentrations of albumin in human interstitial fluid (adipose and muscle) and human serum (36). The concentrations of proteins in different compartment are shown in Table 1 in the main text.

S3.2.2 Equilibrium Association Constants

Equilibrium association constants K_A^P and K_A^{FABP} are used in our model to describe binding of PFAAs to proteins in plasma and interstitial fluid and to FABPs in liver. Albumin constitutes at least half of the proteins in plasma in mammals and is considered an important sink for PFAAs (33,37,38). Although there is no albumin in zebrafish, probably the apoliproprotein A-Ib (about 20% of total plasma proteins in both genders) and other proteins, including vitellogenins, egg yolk precursor proteins which are not observed in human plasma, and hemopexin, perform the same role as albumin in plasma (33). FABPs are abundant in many tissues and have been detected in zebrafish and other fish (39–42). As we could not find fish-specific equilibrium association constants for plasma proteins, we used as a first estimate albumin binding constants for PFOA.

However, reviewed papers related to mammals (43–46) proposed very different values for albumin association constants (from 10^2 to10^6 M^{-1}), for a small number of binding sites, based on different methods (Table S6). The concentration of PFOA in plasma can explain some of this variability. Experiments have shown that the affinity of PFOA-albumin association can increase at lower concentrations of PFOA. On the other hand, the saturation of binding sites can occur when the concentration of PFOA in plasma exceeds the availability of specific binding sites, and consequently a larger number of low affinity binding sites will be occupied (47). Researchers have reported K_{alb} by using different methods, including electrospray ionization, fluorescence, nano-ESI-MS, and equilibrium dialysis. The relative sensitivity of different methods can thus also contribute to observed variability in measured binding affinity.

Table S6. The summary of available methods and values for K_{alb}

Method	Value for K_{alb}	Reference
Electrospray Ionization MS. 19F NMR	$3.7 \times 10^{-}M^{-1}$	(46)
HSA, Fluorescence	$3.7 \times 10^{3}M^{-1}$	(43)
HSA, Fluorescence Sudlow site II,	$40.7 \times 10^{3}M^{-1}$	(44)
BSA, Fluorescence	74×10^{3} M^{-1}	(43)
BSA, nano-ESI-MS	$460 \times 10^{3}M^{-1}$	(45)
BSA, Equilibrium Dialysis	5500×10^{3} M^{-1}	(45)

For PFOA binding to FABPs, we utilized the study by Woodcroft (2010) and Zhang et al. (2013) to estimate association constants (see Table 1 in main text) (48,49).

S3.2.3 Protein-Mediated Hepatobiliary Circulation

Enterohepatic circulation of PFOA has been reported in zebrafish as an important excretory pathway (4). Thus, we consider the hepatobiliary circulation and its role in bioconcentration of PFOA in our model. The hepatobiliary transport of substances from blood to bile involves three steps (Figure S1). First, hepatocytes at the sinusoidal membrane take up various substances from blood. This is followed by intercellular transport and metabolism. Finally, transport of metabolized substances occurs across the apical membrane of hepatocytes into the biliary system

(50). Moreover, the critical role of various membrane transporters has been identified in mammals (51,52). It has been suggested that PFAAs are reabsorbed from the bile back to blood in mammals. However, no data were available for zebrafish, thus we did not consider the reabsorption of PFOA, and assume PFOA is excreted from the bile with a rate that depends on the biliary flow rate and bile concentration of PFOA, $Q_{Bi}C_{Bi}$.

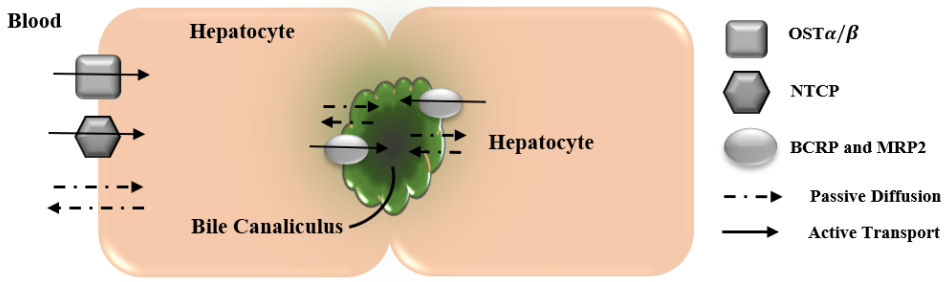

Figure S1. PFOA uptake and elimination in hepatocytes by active transport and passive diffusion

To the best of our knowledge, there are no published studies that measure the transport of PFAAs via enterohepatic circulation in fish. Therefore, we used the results of Zhao et al. (2015) for the rat (53). They investigated the role of transporters in enterohepatic circulation of perfluorooctane sulfonate (PFOS), perfluorohexane sulfonate (PFHxS), and perfluorobutane sulfonate (PFBS). Given the similarity in structure between PFOA and PFOS, the experimental data provided for PFOS were used for modeling PFOA. We consider both passive diffusion and active transport mechanisms in the hepatobiliary circulation of PFOA. Facilitated transport is considered in the liver, where we modeled three competing protein-mediated processes for facilitated transport from blood-liver-bile: PFOA is taken up from the blood to the liver with the help of Sodium/Taurocholate Co-transporting Polypeptide (NTCP) and Organic Solute Transporter α/β (OSTα/β)(53), and removed by the apical sodium-dependent bile salt

transporter (ASBT) from the liver to bile (Figure S1). NTCP and OSTα/β are located in the sinusoidal membrane of hepatocytes and are known to have a direct role in transporting PFAAs from blood to liver. It is known that the bile efflux transporters breast cancer resistance protein (BCRP) and multidrug resistance protein 2 (MRP2), located on the canalicular membrane, interact with PFAAs (54). These transporters facilitate the excretion of xenobiotics from liver into bile. However, we could not find any studies measuring the transport of PFAAs from liver to bile duct. In order to use the result of Zhao et al. (2015), we assumed that ASBT, located in the apical membrane of gut, has the similar role as BCRP and MRP2 (53). We therefore estimated PFOA elimination kinetics by BCRP and MRP2 from liver to bile using ASBT data.

PFOA is removed from the liver to bile (with rate constant b_{clear}) and is transported from blood to liver (with rate constant b_{uptake}). The uptake rates for transporters were converted from mol/mg protein/min to first-order uptake and clearance rate constants, b_{clear} and b_{uptake}. This conversion required the total protein concentration in liver of zebrafish, which we found to be 11.65 μg/mg and 13.45 μg/mg in male and female zebrafish, respectively (55). The average value of protein concentration for the two genders was used as the adult protein concentration in liver. Transport kinetics for the uptake and clearance of PFOA in the liver are shown in Table S7.

Table S7. Flux (J) measured by Zhao et al. (2015) for protein-facilitated uptake and calculated rate constants (b) for clearance and uptake used in our model

	J (mol/mg protein/min)			b_{Uptake} (s^{-1})		b_{Uptake} (s^{-1})	b_{clear} (s^{-1})
	NTCP	OSTα/β	ASBT*	$b_{\text{OST}\alpha/\beta}$($s^{-1}$)	b_{NTCP}(s^{-1})		b_{ASBT}(s^{-1})
Male	0.1×10^{-9}	0.25×10^{-9}	0.03×10^{-9}	5.5×10^{-6}	2.14×10^{-6}	7.64×10^{-6}	6.42×10^{-7}
Female	0.1×10^{-9}	0.25×10^{-9}	0.03×10^{-9}	6.3×10^{-6}	2.47×10^{-6}	8.77×10^{-6}	7.42×10^{-7}
Adult	0.1×10^{-9}	0.25×10^{-9}	0.03×10^{-9}	5.93×10^{-6}	2.3×10^{-6}	8.23×10^{-6}	6.92×10^{-7}

*** ASBT is used as a surrogate for BCRP and MRP2**

S3.3 Passive Diffusion

Three important processes could control the gill uptake rates of neutral organic chemicals from water in fish: ventilation rate (water flow rate across the gills), diffusion (chemical transport across the gill membrane), and perfusion (blood flow rate across gills) (1). Passive diffusion of PFAAs across membranes has been previously reported (56–58). In this model, we assume that passive diffusion of PFOA across cell membranes in the gill of zebrafish (where fatty acid metabolism is not important like other tissues such as gut and liver (59,60)) is the main pathway for uptake of PFOA from water. In other compartments including liver, adipose, muscle, and kidney passive diffusion occurs between blood and interstitial fluid and between interstitial fluid and tissues. Moreover, we considered both passive diffusion and active transport between blood and liver and between liver and bile. In order to measure the passive diffusion, we employed the method applied by Ng and Hungerbühler (2013) based on the empirical study of Weaver et al. (2010) to determine the effective permeability of cell membranes (P_{eff}) to PFOA (1,56). This results in an estimate of P_{eff} of 1.13×10^{-9} m/s. For more information see Ng and Hungerbühler (2013) (1).

It is generally assumed that at steady state the concentration of organic chemicals in the body of fish relative to their concentration in water is the same as the ratio of their uptake and loss rate constants (1). We assumed this applies for the passive diffusion component of PFOA transfer. Thus, by considering the steady-state cell-water concentration ratio (CR_{SS}^{C-w}) from the passive diffusion measurements of Weaver et al. (2010), we could estimate relative rates of uptake and loss via passive diffusion for each tissue, in the same manner as Ng and Hungerbuhler 2013 (1,56). Table S8 lists the parameters associated with passive diffusion of PFOA.

Table S8. Parameters associated with PFOA uptake and loss via the gills

		P_{eff} (m/s)	CR_{SS}^{C-w}	k^{W-B} (m^3/s)	k^{B-W} (m^3/s)
Model	**Male**	1.13×10^{-9}	1.62	9.7×10^{-13}	5.99×10^{-13}
	Female	1.13×10^{-9}	1.62	9.7×10^{-13}	5.99×10^{-13}
	Adult	1.13×10^{-9}	1.62	9.7×10^{-13}	5.99×10^{-13}

S4. Comparing the Availability of Parameters for Zebrafish, Trout, and Rat

To compare the availability of physiological parameters among different species typically used for PBPK models, we have compiled parameters available for rats, rainbow trout, and zebrafish. Table 2 clearly illustrates that nearly all physiological parameters are available for rat and to some extent for trout, while many of them have not been determined for zebrafish (based on major organs such as liver, kidney, adipose, muscle, gill/lung, blood, bile, and gut). Since many studies used immature zebrafish, lack of data is more evident for adult zebrafish. For example, the majority of published studies investigated the bioconcentration of PFAAs in embryo of zebrafish (61–67) and only a few of them studied PFAA bioconcentration in adult zebrafish (4,68–70). Our review of the literature indicates that physiological parameters for zebrafish need more attention if they are to fulfill their promise as ideal model organisms.

Table S10. Comparing the availability of physiological parameters in zebrafish, trout, and rat

Parameters	Organism	Reference
Blood volume of different Tissues	Zebrafish	-------
	Trout	(28,71)
	Rat	(72–75)
Blood flow rate	Zebrafish	(30)
	Trout	(71)
	Rat	(72,74,75)
Fluid volume of different tissues	Zebrafish	-------
	Trout	(20)
	Rat	(76–78)
Concentration of different proteins in both tissue compartment and interstitial fluid	Zebrafish	-------
	Trout	-------
	Rat	(36,46,79–81)
Volume of different tissues	Zebrafish	----------
	Trout	----------
	Rat	(78,82–87)
Surface area of different tissues	Zebrafish	----------
	Trout	----------
	Rat	----------
Gill (lung) ventilation rate	Zebrafish	----------
	Trout	(88)
	Rat	(89)
Biliary flow rate	Zebrafish	----------
	Trout	(31)
	Rat	(75)
Concentration of different proteins in Blood	Zebrafish	(33)
	Trout	(90)
	Rat	(75,91)

S5. Correlation Coefficient Analysis

Correlation analysis between each sampled model parameter and PFOA concentration in all compartments of male, female, and adult zebrafish was performed after 24 days of exposure (Figure S3-S11).

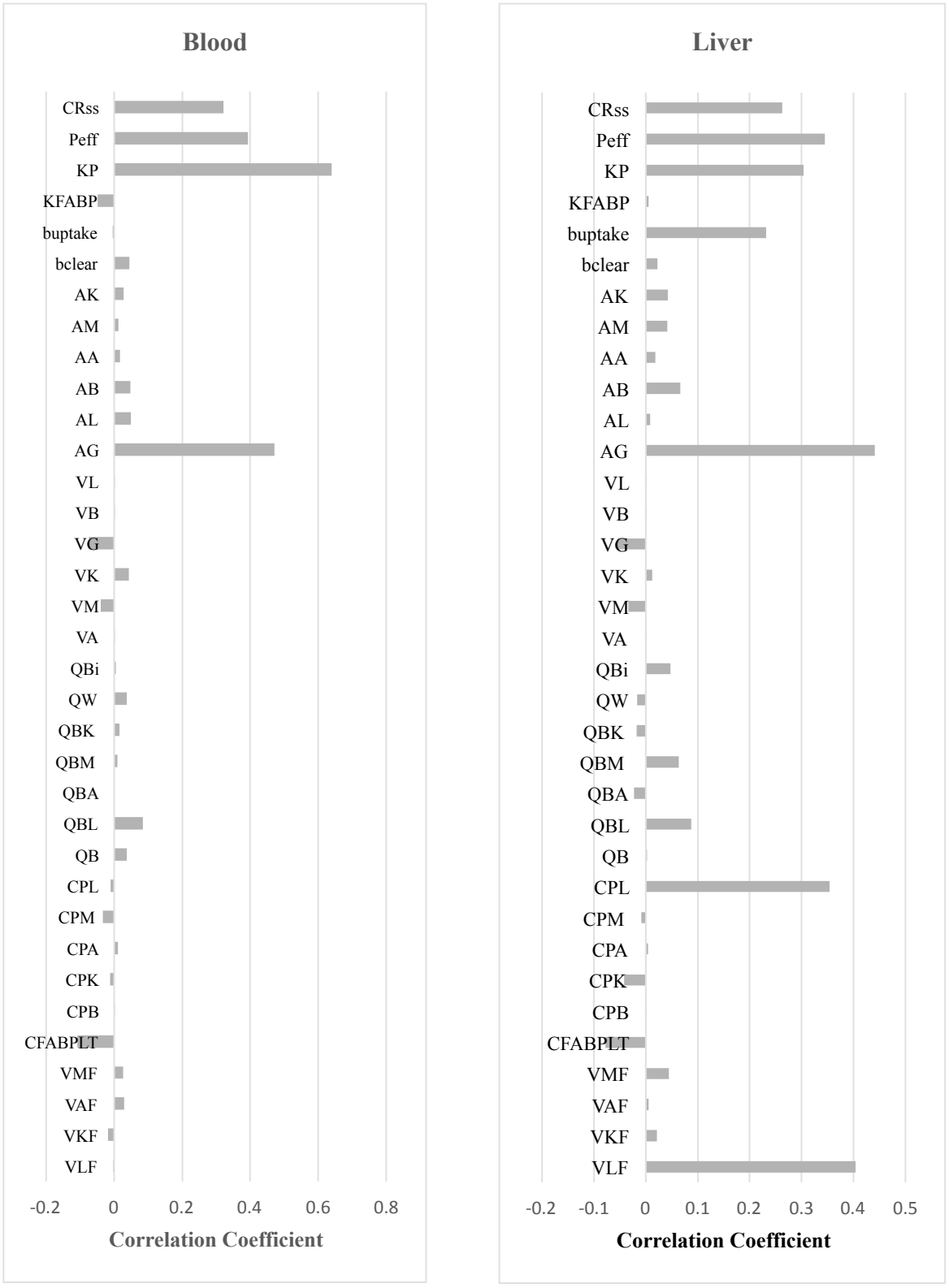

Figure S3. Correlation analysis between each sampled model parameter and PFOA concentration in blood and liver compartments of female zebrafish after 24 days

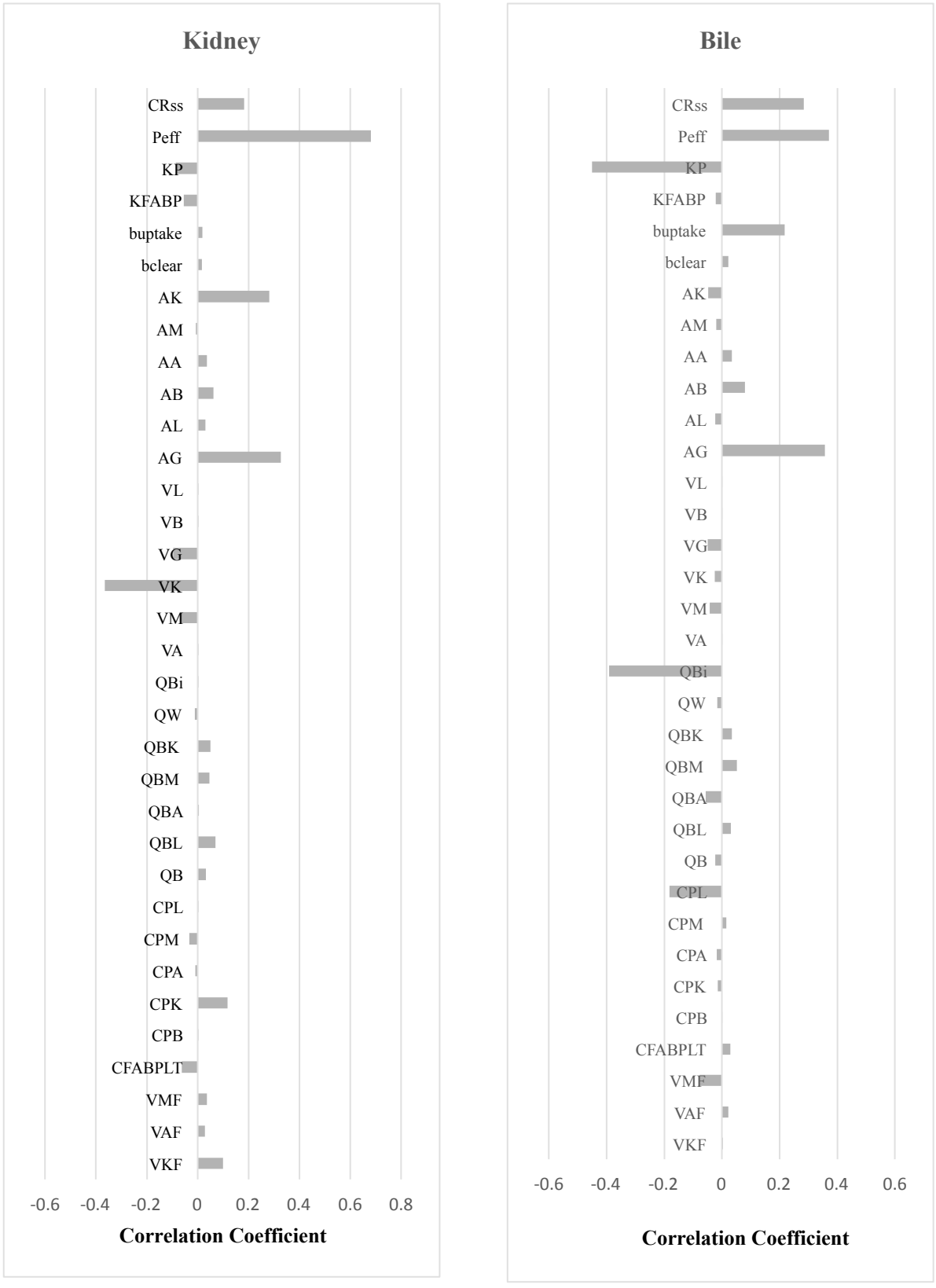

Figure S4. Correlation analysis between each sampled model parameter and PFOA concentration in kidney and bile compartments of female zebrafish after 24 days

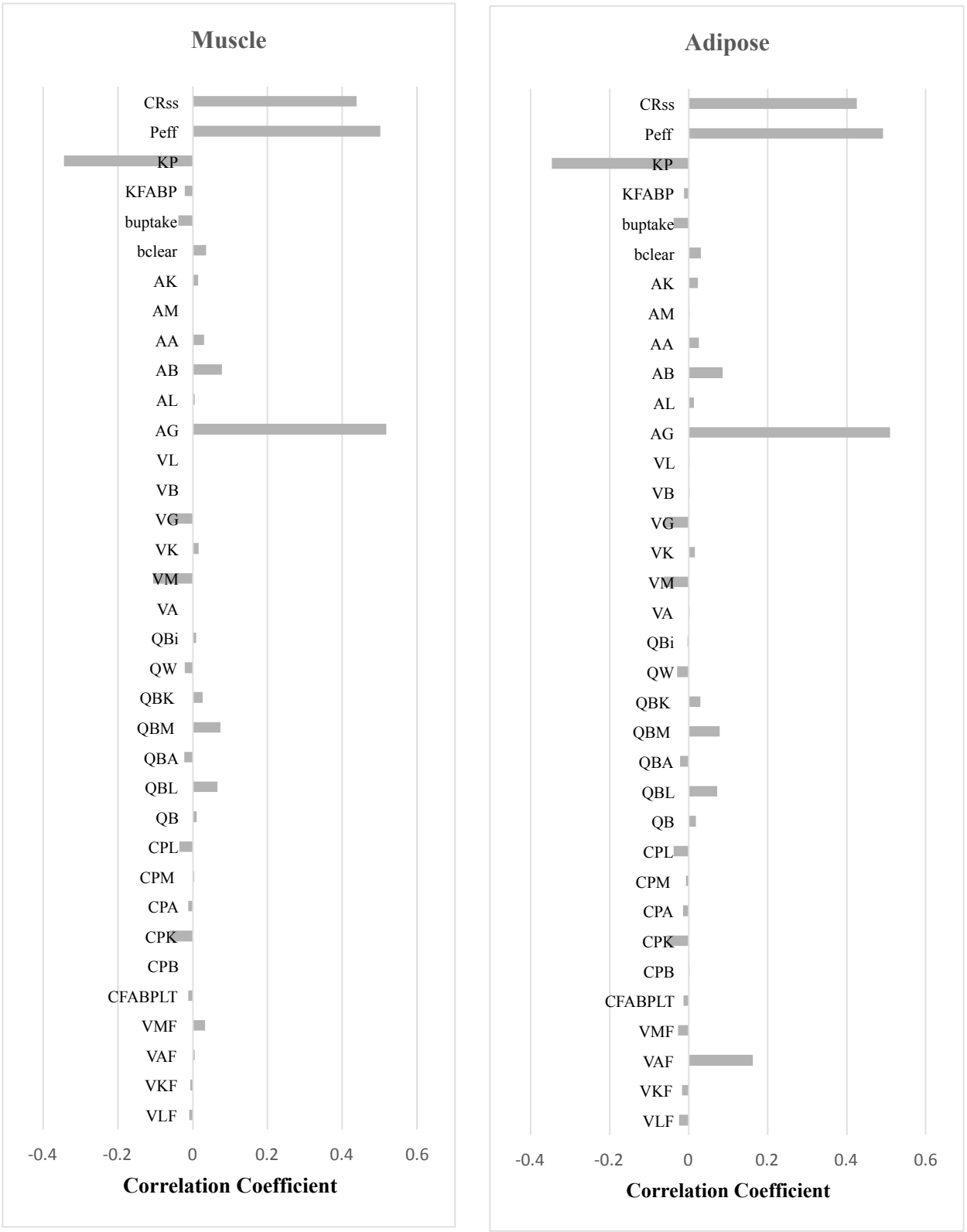

Figure S5. Correlation analysis between each sampled model parameter and PFOA concentration in adipose and muscle compartments of female zebrafish after 24 days

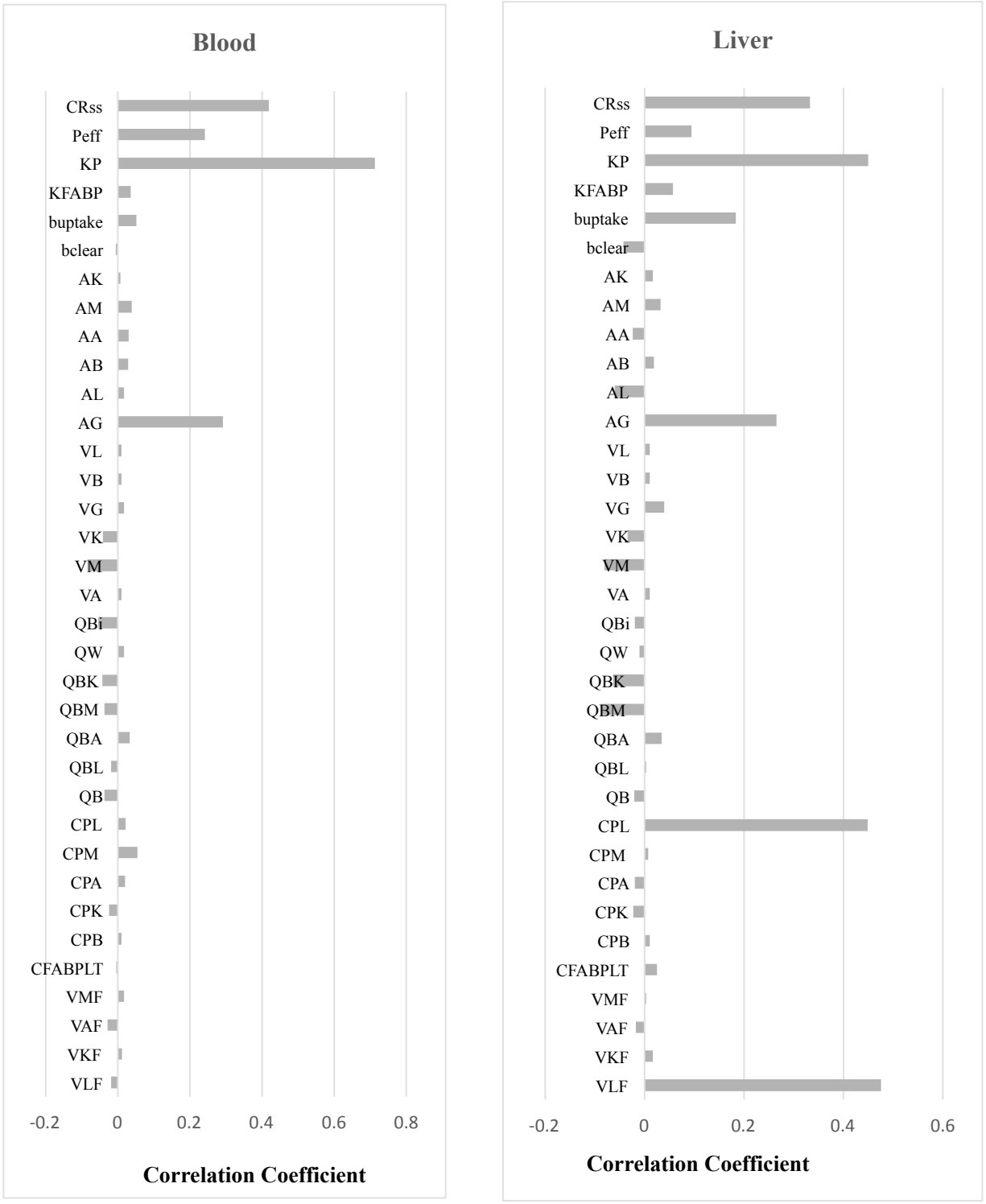

Figure S6. Correlation analysis between each sampled model parameter and PFOA concentration in blood and liver compartments of male zebrafish after 24 days.

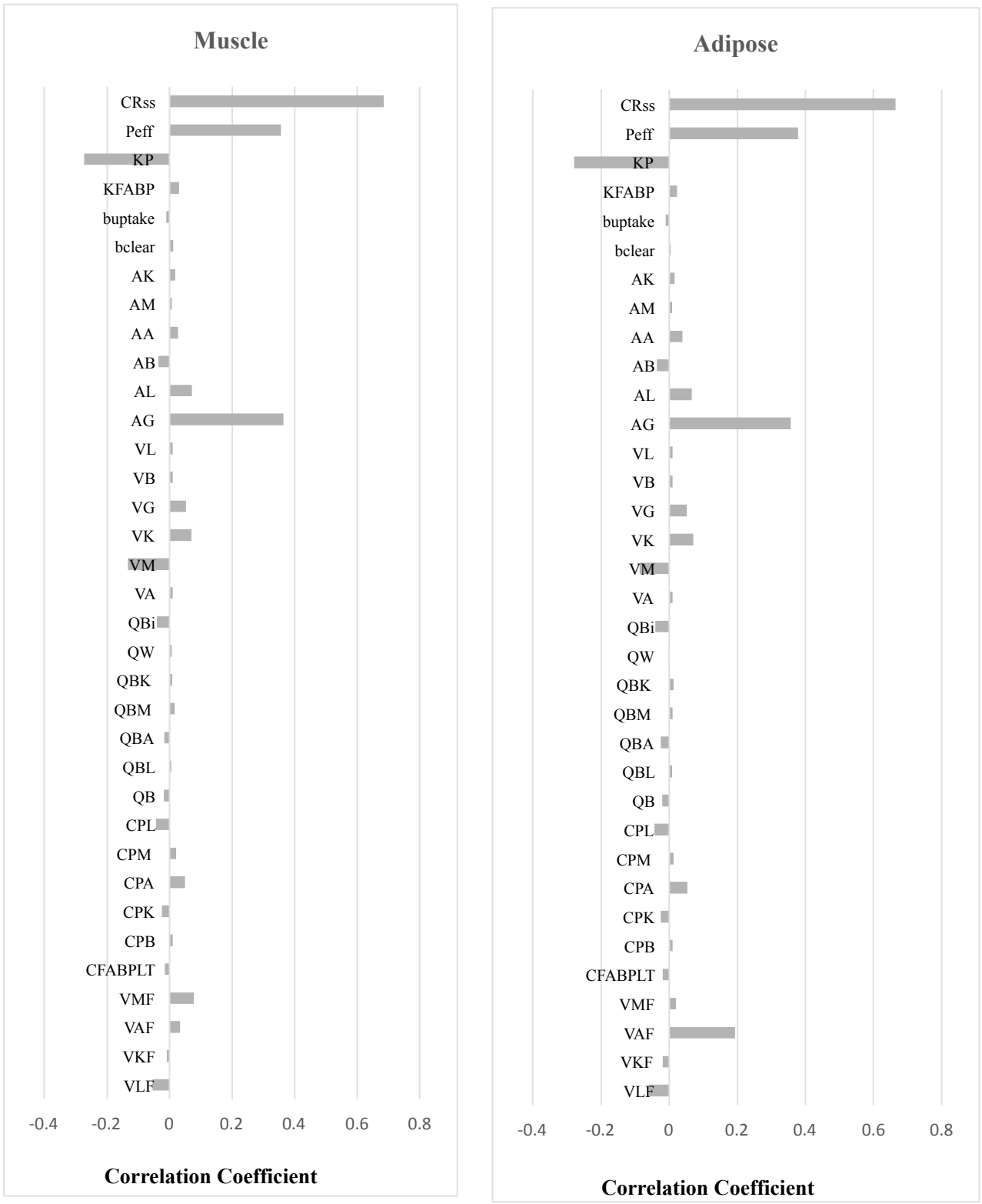

Figure S7. Correlation analysis between each sampled model parameter and PFOA concentration in adipose and muscle compartments of male zebrafish after 24 days

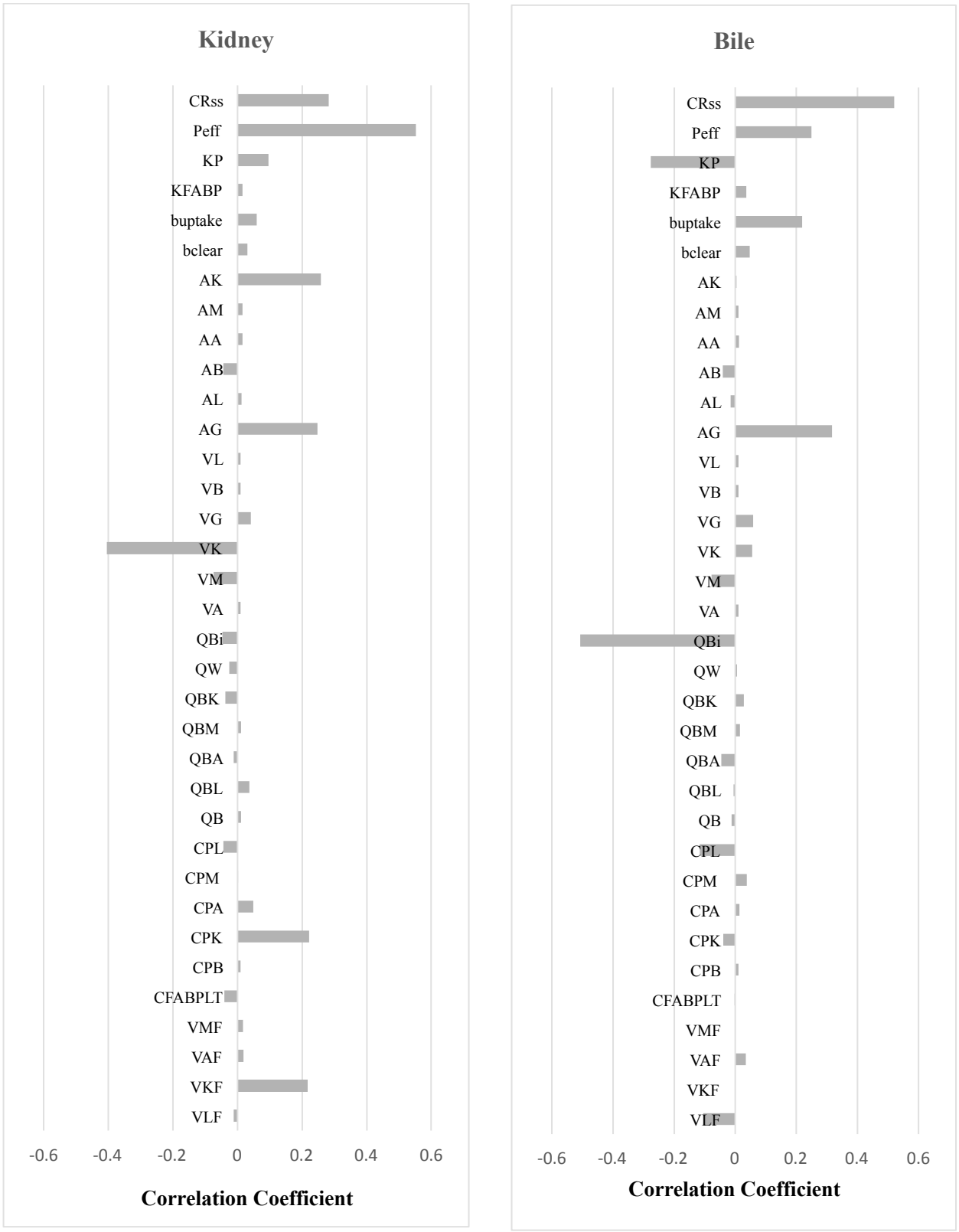

Figure S8. Correlation analysis between each sampled model parameter and PFOA concentration in kidney and bile compartments of male zebrafish after 24 days

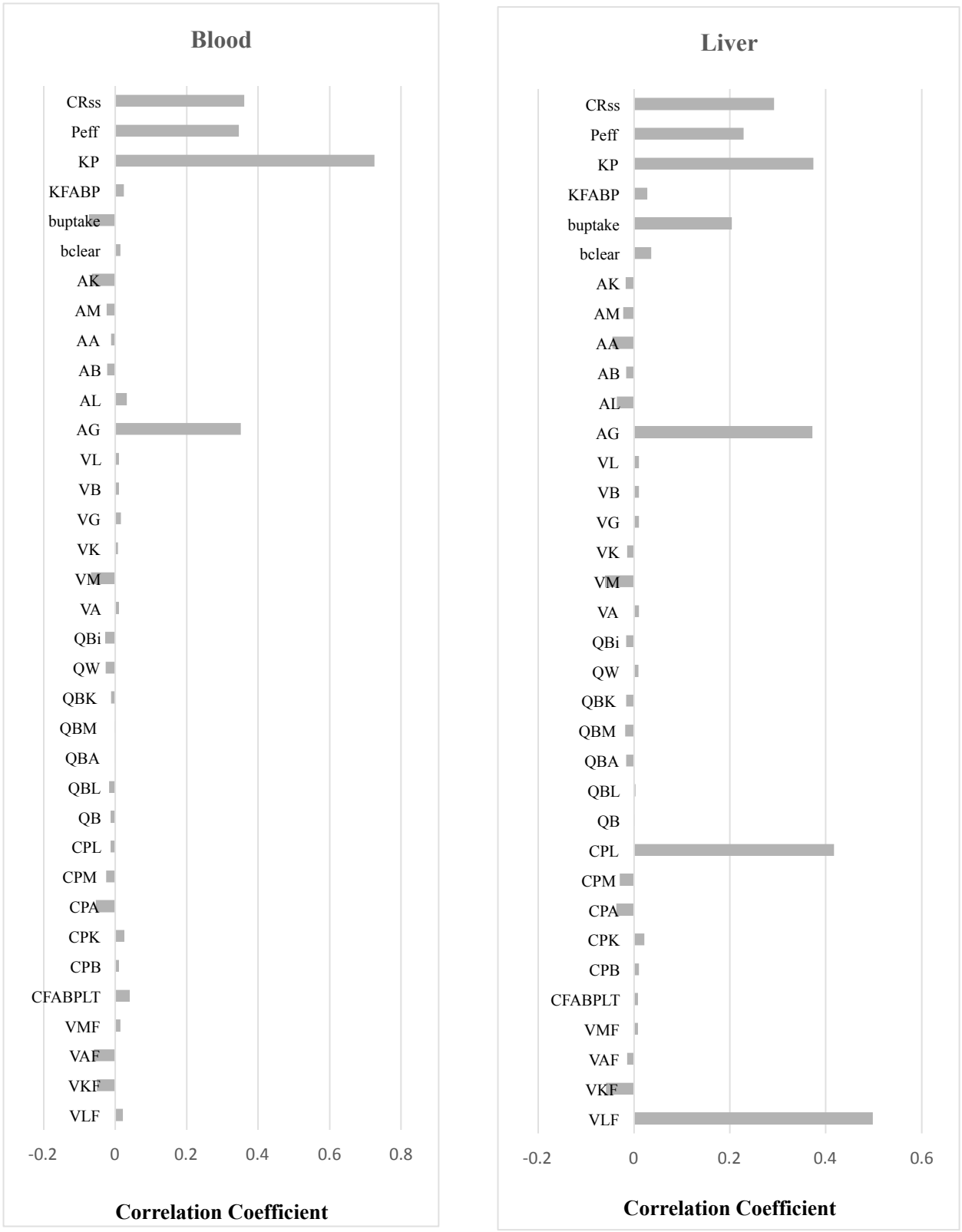

Figure S9. Correlation analysis between each sampled model parameter and PFOA concentration in blood and liver compartments of adult zebrafish after 24 days

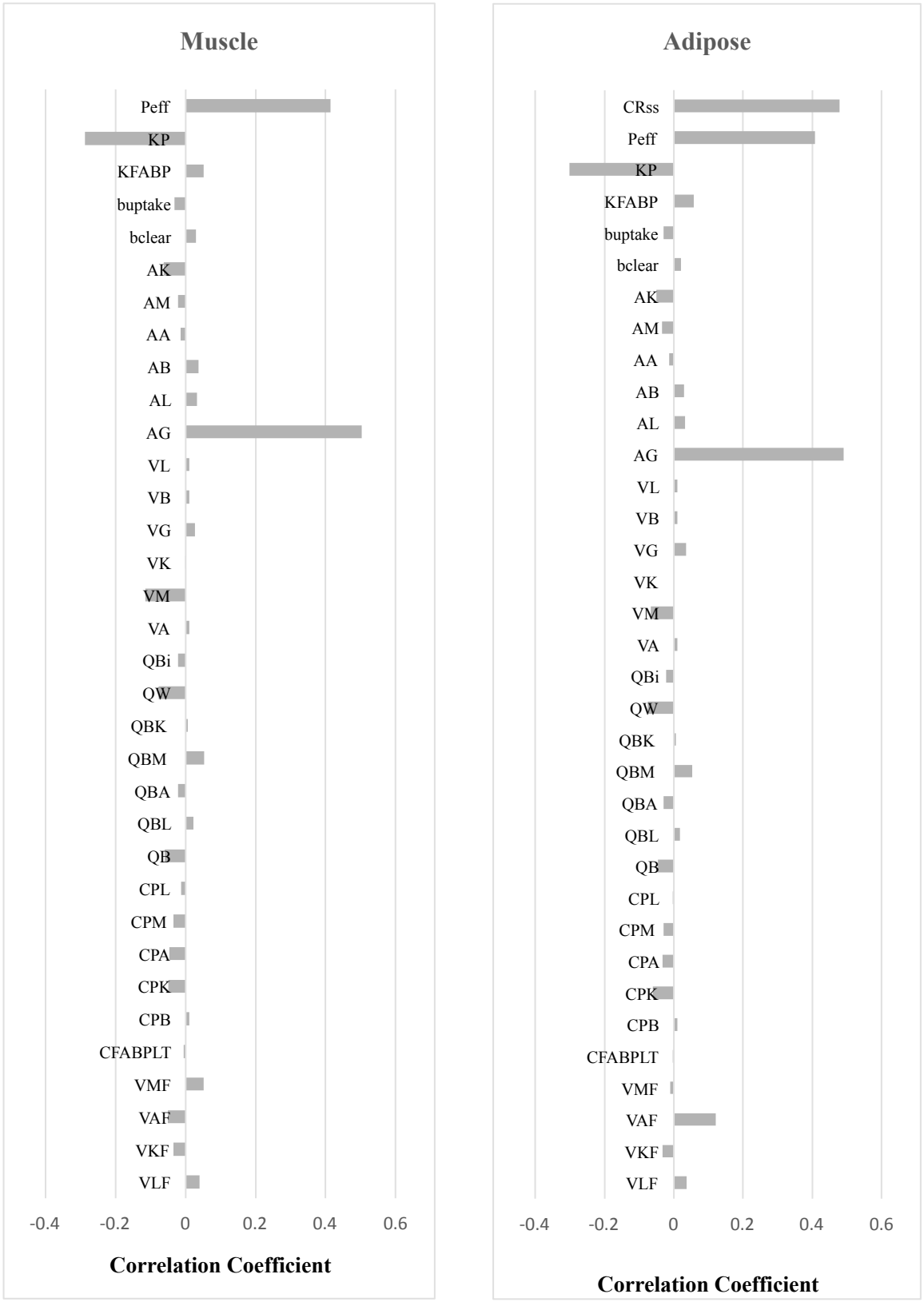

Figure S10. Correlation analysis between each sampled model parameter and PFOA concentration in adipose and muscle compartments of adult zebrafish after 24 days

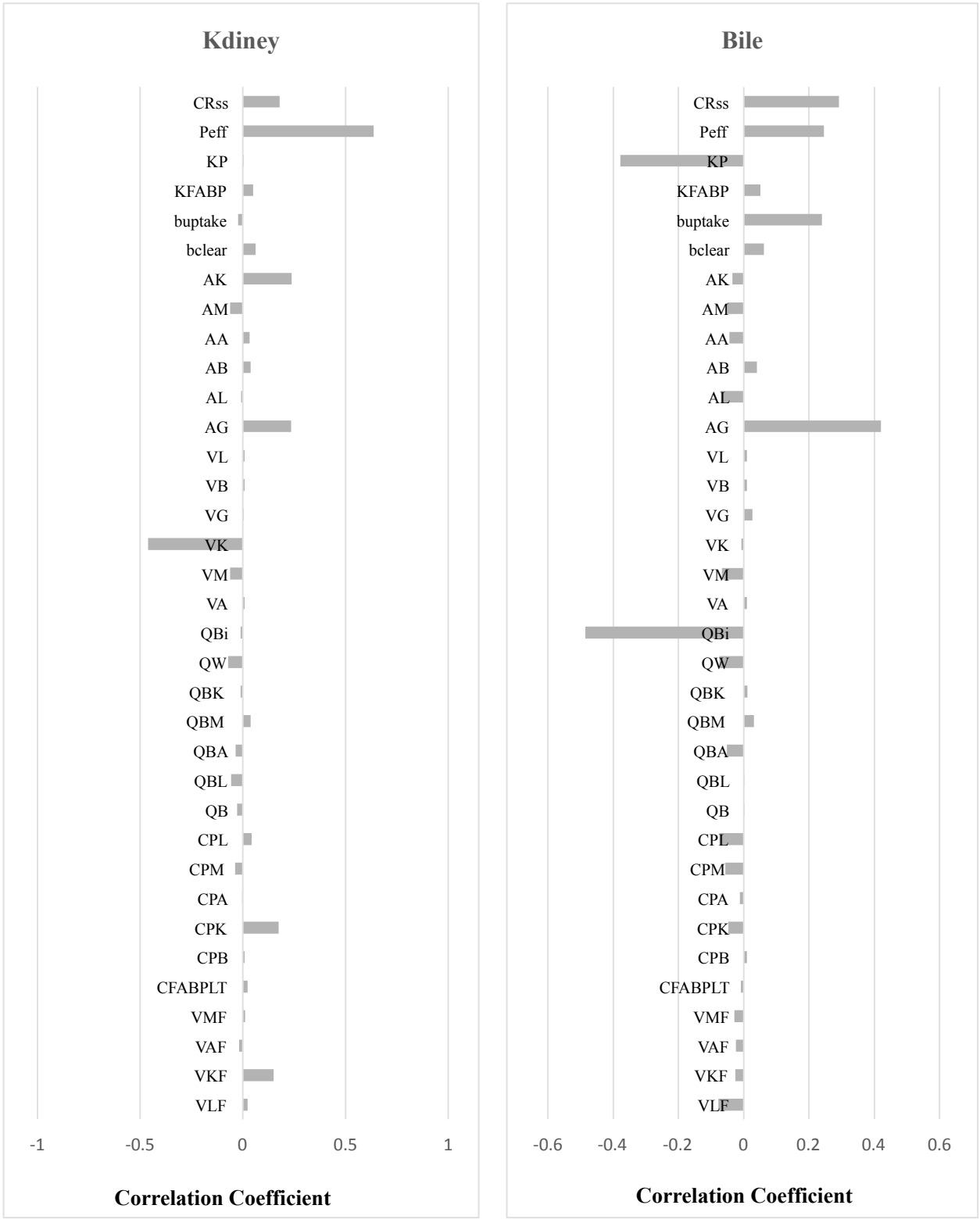

Figure S11. Correlation analysis between each sampled model parameter and PFOA concentration in kidney and bile compartments of adult zebrafish after 24 days

References

1. Ng CA, Hungerbühler K. Bioconcentration of Perfluorinated Alkyl Acids: How Important Is Specific Binding? Environ Sci Technol [Internet]. 2013 Jun 18 [cited 2017 Aug 19];47(13):7214–23. Available from: http://pubs.acs.org/doi/abs/10.1021/es400981a

2. Z.-X. H, M. Z. Toxicokinetic behaviors and modes of perfluorooctane sulfonate (PFOS) and perfluorooctane acid (PFOA) on tilapia (Oreochromis niloticus) [Internet]. Vol. 10, African Journal of Biotechnology. 2011. p. 12943–50. Available from: http://www.academicjournals.org/AJB/PDF/pdf2011/5Oct/Han et al.pdf%5Cnhttp://ovidsp.ovid.com/ovidweb.cgi?T=JS&PAGE=reference&D=emed10&NEWS=N&AN=2011567985

3. Lee JJ, Schultz IR. Sex differences in the uptake and disposition of perfluorooctanoic acid in fathead minnows after oral dosing. Environ Sci Technol. 2010;44(1):491–6.

4. Ulhaq M, Sundström M, Larsson P, Gabrielsson J, Bergman Å, Norrgren L, et al. Tissue uptake, distribution and elimination of 14C-PFOA in zebrafish (Danio rerio). Aquat Toxicol [Internet]. 2015;163:148–57. Available from: http://linkinghub.elsevier.com/retrieve/pii/S0166445X15001095

5. Zhang W, Zhang Y, Zhang H, Wang J, Cui R, Dai J. Sex Differences in Transcriptional Expression of FABPs in Zebrafish Liver after Chronic Perfluorononanoic Acid Exposure. Environ Sci Technol [Internet]. 2012 May [cited 2017 Aug 20];46(9):5175–82. Available from: http://pubs.acs.org/doi/abs/10.1021/es300147w

6. Örn S, Andersson PL, Förlin L, Tysklind M, Norrgren L. The Impact on Reproduction of an Orally Administered Mixture of Selected PCBs in Zebrafish (Danio rerio). Arch Environ Contam Toxicol [Internet]. 1998 Jul 1 [cited 2017 Aug 19];35(1):52–7. Available from: http://link.springer.com/10.1007/s002449900348

7. Lau BYB, Mathur P, Gould GG, Guo S. Identification of a brain center whose activity discriminates a choice behavior in zebrafish. Proc Natl Acad Sci U S A [Internet]. 2011 Feb 8 [cited 2017 Aug 19];108(6):2581–6. Available from: http://www.ncbi.nlm.nih.gov/pubmed/21262817

8. Zang L, Shimada Y, Nishimura Y, Tanaka T, Nishimura N. A Novel, Reliable Method for Repeated Blood Collection from Aquarium Fish. Zebrafish [Internet]. 2013 Sep 29 [cited 2017 Aug 19];10(3):425–32. Available from: http://online.liebertpub.com/doi/abs/10.1089/zeb.2012.0862

9. Ruyra A, Cano-Sarabia M, García-Valtanen P, Yero D, Gibert I, Mackenzie SA, et al. Targeting and stimulation of the zebrafish (Danio rerio) innate immune system with LPS/dsRNA-loaded nanoliposomes. Vaccine [Internet]. 2014 Jun [cited 2017 Aug 19];32(31):3955–62. Available from: http://linkinghub.elsevier.com/retrieve/pii/S0264410X14006665

10. Rey S, Huntingford FA, Boltaña S, Vargas R, Knowles TG, Mackenzie S. Fish can show emotional fever: stress-induced hyperthermia in zebrafish. Proc R Soc London B Biol Sci [Internet]. 2015 [cited 2017 Aug 19];282(1819):20152266. Available from: http://rspb.royalsocietypublishing.org/content/282/1819/20152266

11. Hally AD. A Counting Method for Measuring the Volumes of Tissue Components in Microscopical Sections. Q J Microsc Sci [Internet]. 1964;s3-105(72):503–17. Available from: http://jcs.biologists.org/content/s3-105/72/503.short

12. Regensburg NI, Kok PHB, Zonneveld FW, Baldeschi L, Saeed P, Wiersinga WM, et al. A new and validated CT-Based method for the calculation of orbital Soft tissue volumes. Investig Ophthalmol Vis Sci. 2008;49(5):1758–62.

13. Hevia D, Hevia D, Rodriguez-Garcia A, Alonso-Gervós M, Quirós-González I, Cimadevilla HM, et al. Cell volume and geometric parameters determination in living cells using confocal microscopy and 3D reconstruction. Protoc Exch [Internet]. 2011;1–15. Available from: http://www.nature.com/protocolexchange/protocols/2264

14. Cheng D, Shami GJ, Morsch M, Chung RS, Braet F. Ultrastructural Mapping of the Zebrafish Gastrointestinal System as a Basis for Experimental Drug Studies. Biomed Res Int [Internet]. 2016 Jun 2 [cited 2017 Aug 19];2016:1–13. Available from: http://www.hindawi.com/journals/bmri/2016/8758460/

15. Cecchin D, Negri A, Frigo AC, Bui F, Zucchetta P, Bodanza V, et al. Calculating regional tissue volume for hyperthermic isolated limb perfusion: Four methods compared. Eur J Surg Oncol. 2016;42(12):1898–905.

16. Johnston IA, Bower NI, Macqueen DJ. Growth and the regulation of myotomal muscle mass in teleost fish. J Exp Biol [Internet]. 2011 [cited 2017 Aug 19];214(10):1617–28. Available from: http://jeb.biologists.org/content/214/10/1617.short

17. McCampbell KK, Springer KN, Wingert RA. Atlas of Cellular Dynamics during Zebrafish Adult Kidney Regeneration. Stem Cells Int [Internet]. 2015 May 18 [cited 2017 Aug 19];2015:1–19. Available from: http://www.hindawi.com/journals/sci/2015/547636/

18. Zhou W, Hildebrandt F. Inducible podocyte injury and proteinuria in transgenic zebrafish. J Am Soc Nephrol [Internet]. 2012 Jun 1 [cited 2017 Aug 19];23(6):1039–47. Available from: http://www.ncbi.nlm.nih.gov/pubmed/22440901

19. Hasumura T, Shimada Y, Kuroyanagi J, Nishimura Y, Meguro S, Takema Y, et al. Green tea extract suppresses adiposity and affects the expression of lipid metabolism genes in diet-induced obese zebrafish. Nutr Metab (Lond) [Internet]. 2012 Aug 7 [cited 2017 Aug 28];9(1):73. Available from: http://www.ncbi.nlm.nih.gov/pubmed/22871059

20. Buschnell PG, Conklin DJ, Duff DW, Olson KR. Tissue and whole-body extracellular, red blood cell and albumin spaces in the rainbow trout as a function of time: a reappraisal of the volume of the secondary circulation. J Exp Biol [Internet]. 1998 [cited 2017 Aug 19];201(9):1381–91. Available from: http://jeb.biologists.org/content/201/9/1381.short

21. Soldatov AA. Organ blood flow and vessels of microcirculatory bed in fish. J Evol Biochem Physiol [Internet]. 2006 May [cited 2017 Aug 19];42(3):243–52. Available from: http://link.springer.com/10.1134/S002209300603001X

22. Dubińska-Magiera M, Daczewska M, Lewicka A, Migocka-Patrzałek M, Niedbalska-Tarnowska J, Jagla K. Zebrafish: A Model for the Study of Toxicants Affecting Muscle Development and Function. Int J Mol Sci [Internet]. 2016 Nov 19 [cited 2017 Dec

1];17(11). Available from: http://www.ncbi.nlm.nih.gov/pubmed/27869769

23. Ahuja G, Ivandic I, Saltürk M, Oka Y, Nadler W, Korsching SI. Zebrafish crypt neurons project to a single, identified mediodorsal glomerulus. Sci Rep [Internet]. 2013 [cited 2017 Aug 19];3:2063. Available from: http://www.ncbi.nlm.nih.gov/pubmed/23792970

24. Hanke N, Staggs L, Schroder P, Litteral J, Fleig S, Kaufeld J, et al. "Zebrafishing" for novel genes relevant to the glomerular filtration barrier. Biomed Res Int [Internet]. 2013 Sep 11 [cited 2017 Aug 19];2013:658270. Available from: http://www.ncbi.nlm.nih.gov/pubmed/24106712

25. Biga PR, Goetz FW. Zebrafish and giant danio as models for muscle growth: determinate vs. indeterminate growth as determined by morphometric analysis. Am J Physiol - Regul Integr Comp Physiol [Internet]. 2006 [cited 2017 Aug 19];291(5):R1327–37. Available from: http://ajpregu.physiology.org/content/291/5/R1327.short

26. Imrie D, Sadler KC. White adipose tissue development in zebrafish is regulated by both developmental time and fish size. Dev Dyn [Internet]. 2010 Nov 1 [cited 2017 Aug 19];239(11):3013–23. Available from: http://doi.wiley.com/10.1002/dvdy.22443

27. Grosell M, O'Donnell MJ, Wood CM. Hepatic versus gallbladder bile composition: in vivo transport physiology of the gallbladder in rainbow trout. Am J Physiol - Regul Integr Comp Physiol [Internet]. 2000 [cited 2017 Aug 19];278(6):R1674–84. Available from: http://ajpregu.physiology.org/content/278/6/R1674.short

28. Barron MG, Tarr BD, Hayton WL. Temperature-dependence of cardiac output and regional blood flow in rainbow trout, Salmo gairdneri Richardson. J Fish Biol [Internet]. 1987 Dec 1 [cited 2017 Aug 19];31(6):735–44. Available from: http://doi.wiley.com/10.1111/j.1095-8649.1987.tb05276.x

29. Nichols JW, McKim JM, Andersen ME, Gargas ML, Clewell HJ, Erickson RJ. A physiologically based toxicokinetic model for the uptake and disposition of waterborne organic chemicals in fish. Toxicol Appl Pharmacol [Internet]. 1990 Dec [cited 2017 Aug 16];106(3):433–47. Available from: http://linkinghub.elsevier.com/retrieve/pii/0041008X9090338U

30. Péry ARR, Devillers J, Brochot C, Mombelli E, Palluel O, Piccini B, et al. A Physiologically Based Toxicokinetic Model for the Zebrafish Danio rerio. Environ Sci Technol [Internet]. 2013 Jan 7 [cited 2017 Aug 19];48(1):781–90. Available from: http://pubs.acs.org/doi/abs/10.1021/es404301q

31. Schmidt DC, Weber LJ. Metabolism and Biliary Excretion of Sulfobromophthalein by Rainbow Trout (*Salmo gairdneri*). J Fish Res Board Canada [Internet]. 1973 Sep [cited 2017 Aug 19];30(9):1301–8. Available from: http://www.nrcresearchpress.com/doi/abs/10.1139/f73-210

32. Peters T. All about albumin : biochemistry, genetics, and medical applications [Internet]. Academic Press; 1996 [cited 2017 Aug 19]. 432 p. Available from: https://books.google.com/books?hl=en&lr=&id=i1DC3KlTAB8C&oi=fnd&pg=PP2&dq=All+about+albumin:+biochemistry,+genetics,+and+medical+applications&ots=WXAhdW7vem&sig=3Tkwrd3JcI1IaKWbxLwqLsa-_SE#v=onepage&q=All about albumin%3A

biochemistry%2C genetics%2C and m

33. Li C, Tan XF, Lim TK, Lin Q, Gong Z. Comprehensive and quantitative proteomic analyses of zebrafish plasma reveals conserved protein profiles between genders and between zebrafish and human. Sci Rep [Internet]. 2016;6(April):24329. Available from: http://www.ncbi.nlm.nih.gov/pubmed/27071722%5Cnhttp://www.pubmedcentral.nih.gov/articlerender.fcgi?artid=PMC4829857

34. Londraville RL, Sidell BD. Cold acclimation increases fatty acid-binding protein concentration in aerobic muscle of striped bass, Morone saxatilis. J Exp Zool [Internet]. 1996;275(1):36–44. Available from: http://pinos.cbuc.es:3210/uab?genre=article&sid=ProQ:&atitle=Cold+acclimation+increases+fatty+acid-binding+protein+concentration+in+aerobic+muscle+of+striped+bass%2C+Morone+saxatilis&title=Journal+of+Experimental+Zoology&issn=0022-104X&date=1996-01-01&vol

35. Levitt D. The pharmacokinetics of the interstitial space in humans. BMC Clin Pharmacol [Internet]. 2003 [cited 2017 Aug 30];3(1):3. Available from: https://bmcclinpharma.biomedcentral.com/articles/10.1186/1472-6904-3-3

36. Ellmerer M, Schaupp L, Brunner GA, Sendlhofer G, Wutte A, Wach P, et al. Measurement of interstitial albumin in human skeletal muscle and adipose tissue by open-flow microperfusion. Am J Physiol Endocrinol Metab [Internet]. 2000 Feb [cited 2017 Aug 30];278(2):E352-6. Available from: http://www.ncbi.nlm.nih.gov/pubmed/10662720

37. Weisiger RA. Mechanisms of intracellular fatty acid transport: Role of cytoplasmic-binding proteins. J Mol Neurosci. 2007;33(1):42–4.

38. Hickey NJ, Crump D, Jones SP, Kennedy SW. Effects of 18 perfluoroalkyl compounds on mRNA expression in chicken embryo hepatocyte cultures. Toxicol Sci. 2009;111(2):311–20.

39. Boaru DA, Dragoş N, Schirmer K. Microcystin-LR induced cellular effects in mammalian and fish primary hepatocyte cultures and cell lines: A comparative study. Toxicology. 2006;218(2–3):134–48.

40. Torstensen BE, Nanton DA, Olsvik PA, Sundvold H, Stubhaug I. Gene expression of fatty acid-binding proteins, fatty acid transport proteins (cd36 and FATP) and β-oxidation-related genes in Atlantic salmon (Salmo salar L.) fed fish oil or vegetable oil. Aquac Nutr. 2009;15(4):440–51.

41. Liu RZ, Denovan-Wright EM, Wright JM. Structure, linkage mapping and expression of the heart-type fatty acid-binding protein gene (fabp3) from zebrafish (Danio rerio). Eur J Biochem [Internet]. 2003;270(15):3223–34. Available from: http://www.ncbi.nlm.nih.gov/pubmed/12869198

42. Jordal A-EO, Hordvik I, Pelsers M, Bernlohr D a, Torstensen BE. FABP3 and FABP10 in Atlantic salmon (Salmo salar L.)--general effects of dietary fatty acid composition and life cycle variations. Comp Biochem Physiol B Biochem Mol Biol. 2006;145:147–58.

43. MacManus-Spencer LA, Tse ML, Hebert PC, Bischel HN, Luthy RG. Binding of

perfluorocarboxylates to serum albumin: A comparison of analytical methods. Anal Chem. 2010;82(3):974–81.

44. Chen YM, Guo LH. Fluorescence study on site-specific binding of perfluoroalkyl acids to human serum albumin. Arch Toxicol. 2009;83(3):255–61.

45. Bischel HN, MacManus-Spencer LA, Luthy RG. Noncovalent interactions of long-chain perfluoroalkyl acids with serum albumin. Environ Sci Technol. 2010;44(13):5263–9.

46. Han X, Timothy A. Snow, Raymond A. Kemper A, Jepson GW. Binding of Perfluorooctanoic Acid to Rat and Human Plasma Proteins. Chem Res Toxicol [Internet]. 2003 [cited 2017 Aug 24];16(6):775–81. Available from: http://pubs.acs.org/doi/abs/10.1021/tx034005w?journalCode=crtoec

47. Ng CA, Hungerbühler K. Bioaccumulation of perfluorinated alkyl acids: Observations and models. Vol. 48, Environmental Science and Technology. 2014. p. 4637–48.

48. Woodcroft MW, Ellis DA, Rafferty SP, Burns DC, March RE, Stock NL, et al. Experimental characterization of the mechanism of perfluorocarboxylic acids' liver protein bioaccumulation: The key role of the neutral species. Environ Toxicol Chem [Internet]. 2010 Apr 13 [cited 2017 Aug 20];29(8):n/a-n/a. Available from: http://doi.wiley.com/10.1002/etc.199

49. Zhang L, Ren X-M, Guo L-H. Structure-Based Investigation on the Interaction of Perfluorinated Compounds with Human Liver Fatty Acid Binding Protein. Environ Sci Technol [Internet]. 2013;47(19):11293–301. Available from: http://pubs.acs.org/doi/abs/10.1021/es4026722

50. Nathanson MH, Boyer JL. Mechanisms and regulation of bile secretion. Hepatology [Internet]. 1991 Sep 1 [cited 2017 Aug 19];14(3):551–66. Available from: http://doi.wiley.com/10.1002/hep.1840140324

51. Dawson PA. Role of the intestinal bile acid transporters in bile acid and drug disposition. Vol. 201, Handbook of Experimental Pharmacology. 2011. p. 169–203.

52. Kullak-Ublick GA, Beuers U, Paumgartner G. Hepatobiliary transport. J Hepatol [Internet]. 2000;32(1 Suppl):3–18. Available from: http://ovidsp.ovid.com/ovidweb.cgi?T=JS&PAGE=reference&D=med4&NEWS=N&AN=10728790

53. Zhao W, Zitzow JD, Ehresman DJ, Chang S-C, Butenhoff JL, Forster J, et al. Na^+/Taurocholate Cotransporting Polypeptide and Apical Sodium-Dependent Bile Acid Transporter Are Involved in the Disposition of Perfluoroalkyl Sulfonates in Humans and Rats. Toxicol Sci [Internet]. 2015 Aug 1 [cited 2017 Aug 19];146(2):363–73. Available from: https://academic.oup.com/toxsci/article-lookup/doi/10.1093/toxsci/kfv102

54. Köck K, Brouwer KLR. A Perspective on Efflux Transport Proteins in the Liver. Clin Pharmacol Ther [Internet]. 2012;92(5):599–612. Available from: http://doi.wiley.com/10.1038/clpt.2012.79

55. Begam Shamshad S, Suvarchala G, Philip G. Philip et al., PROTEIN PROFILE IN TISSUES OF ZEBRAFISH EXPOSED TO DELTAMETHRIN. J BioInnovation.

2016;5(6):914–22.

56. Weaver YM, Ehresman DJ, Butenhoff JL, Hagenbuch B. Roles of Rat Renal Organic Anion Transporters in Transporting Perfluorinated Carboxylates with Different Chain Lengths. Toxicol Sci [Internet]. 2010 Feb 1 [cited 2017 Aug 20];113(2):305–14. Available from: https://academic.oup.com/toxsci/article/1676945/Roles

57. Yang C-H, Glover KP, Han X. Characterization of Cellular Uptake of Perfluorooctanoate via Organic Anion-Transporting Polypeptide 1A2, Organic Anion Transporter 4, and Urate Transporter 1 for Their Potential Roles in Mediating Human Renal Reabsorption of Perfluorocarboxylates. Toxicol Sci [Internet]. 2010 Oct [cited 2017 Sep 16];117(2):294–302. Available from: http://www.ncbi.nlm.nih.gov/pubmed/20639259

58. Han X, Yang C, Snajdr S, Nabb D, Mingoia R. Uptake of perfluorooctanoate in freshly isolated hepatocytes from male and female rats. Toxicol Lett [Internet]. 2008 Sep 26 [cited 2017 Sep 16];181(2):81–6. Available from: http://www.ncbi.nlm.nih.gov/pubmed/18662756

59. Her GM, Chiang C-C, Wu J-L. Zebrafish intestinal fatty acid binding protein (I-FABP) gene promoter drives gut-specific expression in stable transgenic fish. genesis [Internet]. 2004 Jan [cited 2017 Dec 1];38(1):26–31. Available from: http://www.ncbi.nlm.nih.gov/pubmed/14755801

60. Her GM, Chiang C-C, Chen W-Y, Wu J-L. In vivo studies of liver-type fatty acid binding protein (L-FABP) gene expression in liver of transgenic zebrafish (Danio rerio). FEBS Lett [Internet]. 2003 Mar 13 [cited 2017 Dec 1];538(1–3):125–33. Available from: http://www.ncbi.nlm.nih.gov/pubmed/12633865

61. Du Y, Shi X, Yu K, Liu C, Zhou B. Chronic effects of waterborne PFOS exposure on growth, development, reproduction and hepatotoxicity in Zebrafish. Interdiscip Stud [Internet]. 2008 [cited 2017 Aug 19];3. Available from: https://www.terrapub.co.jp/onlineproceedings/ec/01/pdf/BRCP05.pdf

62. Shi X, Yeung LWY, Lam PKS, Wu RSS, Zhou B. Protein Profiles in Zebrafish (Danio rerio) Embryos Exposed to Perfluorooctane Sulfonate. Toxicol Sci [Internet]. 2009 Aug 1 [cited 2017 Aug 19];110(2):334–40. Available from: https://academic.oup.com/toxsci/article-lookup/doi/10.1093/toxsci/kfp111

63. Huang H, Huang C, Wang L, Ye X, Bai C, Simonich MT, et al. Toxicity, uptake kinetics and behavior assessment in zebrafish embryos following exposure to perfluorooctanesulphonicacid (PFOS). Aquat Toxicol [Internet]. 2010 Jun [cited 2017 Aug 19];98(2):139–47. Available from: http://linkinghub.elsevier.com/retrieve/pii/S0166445X10000433

64. Zheng X-M, Liu H-L, Shi W, Wei S, Giesy JP, Yu H-X. Effects of perfluorinated compounds on development of zebrafish embryos. Environ Sci Pollut Res [Internet]. 2012 Aug 31 [cited 2017 Aug 19];19(7):2498–505. Available from: http://link.springer.com/10.1007/s11356-012-0977-y

65. Ulhaq M, Örn S, Carlsson G, Morrison DA, Norrgren L. Locomotor behavior in zebrafish (Danio rerio) larvae exposed to perfluoroalkyl acids. Aquat Toxicol [Internet]. 2013 Nov

[cited 2017 Aug 19];144:332–40. Available from: http://linkinghub.elsevier.com/retrieve/pii/S0166445X13002907

66. Ding G, Zhang J, Chen Y, Wang L, Wang M, Xiong D, et al. Combined Effects of PFOS and PFOA on Zebrafish (Danio rerio) Embryos. Arch Environ Contam Toxicol [Internet]. 2013 May 12 [cited 2017 Aug 19];64(4):668–75. Available from: http://link.springer.com/10.1007/s00244-012-9864-2

67. Liu H, Sheng N, Zhang W, Dai J. Toxic effects of perfluorononanoic acid on the development of Zebrafish (Danio rerio) embryos. J Environ Sci [Internet]. 2015 Jun [cited 2017 Aug 19];32:26–34. Available from: http://linkinghub.elsevier.com/retrieve/pii/S1001074215000935

68. Sharpe RL, Benskin JP, Laarman AH, MacLeod SL, Martin JW, Wong CS, et al. Perfluorooctane sulfonate toxicity, isomer-specific accumulation, and maternal transfer in zebrafish (Danio rerio) and rainbow trout (Oncorhynchus mykiss). Environ Toxicol Chem. 2010;29(9):1957–66.

69. Zhang W, Sheng N, Wang M, Zhang H, Dai J. Zebrafish reproductive toxicity induced by chronic perfluorononanoate exposure. Aquat Toxicol [Internet]. 2016;175:269–76. Available from: http://dx.doi.org/10.1016/j.aquatox.2016.04.005

70. Chen F, Gong Z, Kelly BC. Bioavailability and bioconcentration potential of perfluoroalkyl-phosphinic and -phosphonic acids in zebrafish (Danio rerio): Comparison to perfluorocarboxylates and perfluorosulfonates. Sci Total Environ [Internet]. 2016 Oct [cited 2017 Sep 4];568:33–41. Available from: http://linkinghub.elsevier.com/retrieve/pii/S0048969716311524

71. Gingerich W., Pityer R., Rach J. Estimates of plasma, packed cell and total blood volume in tissues of the rainbow trout (Salmo gairdneri). Comp Biochem Physiol Part A Physiol [Internet]. 1987 Jan [cited 2017 Aug 19];87(2):251–6. Available from: http://linkinghub.elsevier.com/retrieve/pii/0300962987901198

72. Everett NB, Simmons B, Lasher EP. Distribution of blood (Fe 59) and plasma (I 131) volumes of rats determined by liquid nitrogen freezing. Circ Res [Internet]. 1956 Jul [cited 2017 Sep 25];4(4):419–24. Available from: http://www.ncbi.nlm.nih.gov/pubmed/13330185

73. Sakaeda T, Fukumura K, Takahashi K, Matsumura S, Matsuura E, Hirano K. Blood flow rate in normal and tumor-bearing rats in conscious state, under urethane anesthesia, and during systemic hypothermia. J Drug Target. 1998;6(4):261–72.

74. Brown RP, Delp MD, Lindstedt SL, Rhomberg LR, Beliles RP. Physiological Parameter Values for Physiologically Based Pharmacokinetic Models. Toxicol Ind Health [Internet]. 1997;13(4):407–84. Available from: http://journals.sagepub.com/doi/10.1177/074823379701300401

75. Davies B, Morris T. Physiological parameters in laboratory animals and humans. Vol. 10, Pharmaceutical Research. 1993. p. 1093–5.

76. Barratt TM, Walser M. Extracellular fluid in individual tissues and in whole animals: the

distribution of radiosulfate and radiobromide. J Clin Invest. 1969;48(1):56–66.

77. LARSON M, SJÖQUIST M, WOLGAST M. Renal interstitial volume of the rat kidney. Acta Physiol Scand. 1984;120(2):297–304.

78. Blouin A, Bolender RP, Weibel ER. Distribution of organelles and membranes between hepatocytes and nonhepatocytes in the rat liver parenchyma. A stereological study. J Cell Biol. 1977;72(2):441–55.

79. Ockner RK, Manning JA, Kane JP. Fatty acid binding protein. Isolation from rat liver, characterization, and immunochemical quantification. J Biol Chem. 1982;257(13):7872–8.

80. Kimura H, Odani S, Nishi S, Sato H, Arakawa M, Ono T. Primary structure and cellular distribution of two fatty acid-binding proteins in adult rat kidneys. J Biol Chem. 1991;266(9):5963–72.

81. Maatman RG, van de Westerlo EM, van Kuppevelt TH, Veerkamp JH. Molecular identification of the liver- and the heart-type fatty acid-binding proteins in human and rat kidney. Use of the reverse transcriptase polymerase chain reaction. Biochem J [Internet]. 1992 Nov 15 [cited 2017 Sep 25];288 (Pt 1):285–90. Available from: http://www.ncbi.nlm.nih.gov/pubmed/1280113

82. Qin Y, Van Cauteren M, Osteaux M, Willems G. Determination of liver volume in vivo in rats using MRI. Eur J Radiol. 1990;11(3):191–5.

83. Ross R, Léger L, Guardo R, De Guise J, Pike BG. Adipose tissue volume measured by magnetic resonance imaging and computerized tomography in rats. J Appl Physiol. 1991;70(5):2164–72.

84. Strømmen K, Stormark TA, Iversen BM, Matre K. Volume estimation of small phantoms and rat kidneys using three-dimensional ultrasonography and a position sensor. Ultrasound Med Biol. 2004;30(9):1109–17.

85. McConnell EL, Basit AW, Murdan S. Measurements of rat and mouse gastrointestinal pH, fluid and lymphoid tissue, and implications for in-vivo experiments. J Pharm Pharmacol [Internet]. 2008;60(1):63–70. Available from: http://doi.wiley.com/10.1211/jpp.60.1.0008

86. Kuethe DO, Behr VC, Begay S. Volume of rat lungs measured throughout the respiratory cycle using 19F NMR of the inert gas SF6. Magn Reson Med. 2002;48(3):547–9.

87. Mele A, Fonzino A, Rana F, Camerino GM, De Bellis M, Conte E, et al. In vivo longitudinal study of rodent skeletal muscle atrophy using ultrasonography. Sci Rep [Internet]. 2016;6:20061. Available from: http://www.pubmedcentral.nih.gov/articlerender.fcgi?artid=4735519&tool=pmcentrez&rendertype=abstract

88. Erickson RJ, McKim JM, Lien GJ, Hoffman AD, Batterman SL. Uptake and elimination of ionizable organic chemicals at fish gills: I. Model formulation, parameterization, and behavior. Environ Toxicol Chem. 2006;25(6):1512–21.

89. Strohl KP, Thomas a J, St Jean P, Schlenker EH, Koletsky RJ, Schork NJ. Ventilation and metabolism among rat strains. J Appl Physiol [Internet]. 1997;82(1):317–23. Available

from: http://www.ncbi.nlm.nih.gov/pubmed/9029232

90. Manera M, Britti D. Assessment of blood chemistry normal ranges in rainbow trout. J Fish Biol. 2006;69(5):1427–34.

91. Crisman TS, Claffey KP, Saouaf R, Hanspal J, Brecher P. Measurement of rat heart fatty acid binding protein by ELISA. Tissue distribution, developmental changes and subcellular distribution. J Mol Cell Cardiol. 1987;19(5):423–31.